Crossover in the XY model from three to two dimensions

Wolfhard Janke and Tetsuo Matsui
Institut für Theoretische Physik, Freie Universität Berlin, D-1000 Berlin 33, Germany
(Received 26 March 1990)

We study the crossover between two- and three-dimensional behaviors of the Villain form of the XY spin model on a three-dimensional lattice with anisotropic couplings $J_1=J_2=J$, $J_3=\alpha J$ ($0\le\alpha\le 1$). The α dependence of various quantities is examined by means of duality transformations, Migdal renormalization group, and Monte Carlo simulations. For the specific heat, a crossover into the Kosterlitz-Thouless behavior takes place around $\alpha\simeq 0.2$, which corresponds to $\alpha_{\cos}\simeq 0.015$ in the cosine form of the XY model. Some implications for models of high-T_c superconductivity are discussed.

I. INTRODUCTION

Various kinds of experiments on high-T_c superconductors have exhibited that the relevant structure of these materials are layers of two-dimensional Cu-O planes. Holes (or electrons) at each site have short-range hopping interactions within the plane. In addition, there are weak but finite couplings between the layers. There are claims[1] reporting that the superconducting phase transition is of Kosterlitz-Thouless (KT) type,[2] a characteristic phase transition available in pure two dimensions. They are based on the observations of the KT behaviors in electric transport properties mainly in the temperature interval (~ 0.2–3.0 K) between $T_{\rm KT}$ (KT critical temperature) and $T_{\rm GL}$ (Ginzburg-Landau mean-field critical temperature).[1] Some authors consider the possibility that flux vortices in the conventional theory might engage in the KT behaviors, while others speculate that yet unknown novel objects might be invoked in explanations.[1] It should be pointed out that all these experiments do not rule out genuine three-dimensional (3D) critical behaviors that might still appear in the very vicinity of the transition temperature T_c.

Still, most theoretical approaches to high-T_c phenomena work with models defined on the two-dimensional (2D) lattice explicitly. To consider these as realistic models it would be necessary to evaluate the effects of the weak interplane couplings mentioned above, since, as is well known, the dimensionality of the system is crucial for determining the universality class of its normal super phase transition. Such an evaluation would be useful to check the consistency not only of models themselves but also of assumptions employed in theoretical and experimental analyses.

In this paper we study the effect of such anisotropic coupling ($\equiv\alpha$) in the context of the classical XY spin model by using various methods available. We choose the XY model, since it is the canonical representation with local interactions exhibiting the KT transition in two dimensions. Apart from its close relation to the high-T_c phenomena, such a study is also of interest from the view point of the statistical mechanics of topological excitations. In two dimensions ($\alpha=0$) the system is equivalent to an ensemble of pointlike vortices with logarithmic interaction, while in three dimensions ($\alpha=1$) it can be described as an ensemble of vortex loops, with parallel line elements interacting via the usual Coulomb potential $\propto 1/r$. What is happening in the intermediate region of α? To investigate this question we choose in this paper the Villain form of the XY model,[3] instead of the cosine form, since it is known that topological excitations and spin waves are simply decoupled in the Villain form.

In 2D the XY system exhibits a KT transition that is characterized by its smoothness (being formally of infinite order). There appear no long-range orders nor singularities in thermodynamic quantities for zero external fields. The transition point $T_{\rm KT}$ is located by an exponential divergence of the correlation length ξ and the susceptibility χ at $\beta\equiv 1/T\simeq 0.73$ (Ref. 4) [or, in the cosine model, at $\beta_{\cos}=1.114\pm 0.003$ (Ref. 5)]. More precisely, approaching $T_{\rm KT}$ from high temperatures, the correlation length ξ and the susceptibility χ exhibit the KT behavior[2]

$$\xi\simeq\exp\left[\frac{b_\xi}{\sqrt{T-T_{\rm KT}}}\right],\quad b_\xi\simeq 1.7\ ,$$
$$\chi\simeq\xi^{2-\eta},\quad \eta\simeq\tfrac{1}{4}\ . \tag{1}$$

For low temperatures, $T<T_{\rm KT}$, both ξ and χ stay infinite. The specific heat C, on the other hand, develops only a very smooth, finite peak located about 20% higher in temperature than $T_{\rm KT}$.[6]

In 3D the system exhibits a second-order transition at $\beta\simeq 0.33$ (Refs. 7 and 8) [$\beta_{\cos}=0.4539$ (Ref. 9)] where the correlation length and the susceptibility diverge, and the specific heat develops a cusplike singularity with a jump, as in the λ transition of liquid helium.[10] The critical behavior can be described by power laws,

$$\xi\simeq|T-T_c|^{-\nu},\quad \nu=0.669\pm 0.002\ , \tag{2a}$$
$$\chi\simeq|T-T_c|^{-\gamma},\quad \gamma=1.316\pm 0.0025\ , \tag{2b}$$

where we have taken the critical exponents ν and γ from the standard renormalization group calculation.[11] Ap-

plying the scaling relation $\alpha_C=2-Dv$, this implies for the specific heat C of the 3D XY model a negative exponent α_C (which should not be confused with our anisotropy parameter α),

$$C\simeq|T-T_c|^{-\alpha_C},\quad \alpha_C=-0.007\pm0.006\ , \tag{3}$$

showing that C remains finite at T_c. Note that due to this property the maximum of C can, in principle, be displaced from the location of the cusp. In the low-temperature phase, the magnetization m develops according to[11]

$$m\simeq|T-T_c|^{\beta},\quad \beta=0.3455\pm0.020\ . \tag{4}$$

It is quite interesting to imagine how the two trajectories, the maximum of C and the peak of χ, vary as functions of α from three dimensions to two dimensions. Are they separated from the beginning (at three dimensions)? Or do they move together until just the end at two dimensions, and then jump discontinuously at two dimensions? We will see below that the most natural case is the following: The cusp of C is always accompanied with the χ singularity. The power-law behavior of C near the cusp at three-dimensions exists for all $\alpha\neq0$ and is converted into the essential singularity as $\simeq\exp[-b_C/\sqrt{T-T_{\rm KT}}]$ at two dimensions ($\alpha=0$). Due to the finiteness of C, the maximum of C can deviate more and more from the location of the cusp, thus tracing its own trajectory with decreasing α and ending up with a 20% deviation at two dimensions.

The paper is organized as follows. In Sec. II, the Villain model and its topological representation are introduced. In Sec. III, several theoretical analyses are collected. In Sec. IV, the results of Monte Carlo (MC) simulations are given. Section V is devoted to discussions.

II. MODEL AND VORTEX-LOOP REPRESENTATION

The partition function Z of the Villain form of the anisotropic XY model is given by

$$Z=\sum_{\{n_i\}}\left[\prod_x\int_{-\pi}^{\pi}d\theta(x)/2\pi\right]\exp(-S_V)\ , \tag{5}$$

$$S_V=\frac{\beta}{2}\sum_x[(\nabla_1\theta-2\pi n_1)^2+(\nabla_2\theta-2\pi n_2)^2+\alpha(\nabla_3\theta-2\pi n_3)^2]\ ,$$

where $x=(x_1,x_2,x_3)\in\mathbb{Z}^3$ are the sites of a three-dimensional cubic lattice, and $i(=1,2,3)$ denote the directions. The angles $\theta(x)$ parametrize O(2) spins $\mathbf{s}(x)=(\cos\theta(x),\sin\theta(x))$, the lattice gradients are $\nabla_i\theta(x)\equiv\theta(x+i)-\theta(x)$, and the integer variables n_i sit on the links $(x,x+i)$. The parameter β is the inverse temperature times the exchange coupling constant $J\equiv J_1=J_2$, and $\alpha\equiv J_3/J$ measures the anisotropy of (1,2) plane versus 3 direction. Note that the case $\alpha=1$ reproduces the correct 3D expression, while the case $\alpha=0$ gives rise to a set of independent layers, each of which is described by the 2D model.

Now we follow the standard method of duality transformation.[12] The periodic Gaussian factors in (5) have the Gaussian Fourier components

$$\sum_{n\in\mathbb{Z}}\exp[-\tfrac{1}{2}\beta(\varphi-2\pi n)^2]=\sum_{b\in\mathbb{Z}}f_V(b)\exp(ib\varphi)\ ,\qquad f_V(b)=(2\pi\beta)^{-1/2}\exp[-b^2/2\beta]\ . \tag{6}$$

The integration over θ yields

$$Z=C\sum_{\{b_i\}}\prod_x\delta_{\bar\nabla_i b_i,0}\exp[-S(b)]\ ,\qquad C=\prod_x(2\pi\beta)^{-3/2}\alpha^{-1/2}\ ,\qquad S(b)=(2\beta)^{-1}\sum_x[b_1^2+b_2^2+\alpha^{-1}b_3^2]\ . \tag{7}$$

The constraints $\bar\nabla_i b_i(x)\equiv\sum_i[b_i(x)-b_i(x-i)]=0$ are solved by introducing the *integer*-valued gauge field a_i through

$$b_i=\epsilon_{ijk}\nabla_j a_k(x+i)\ . \tag{8}$$

Z now takes the form of a sum over a_i, which is rewritten by the Poisson summation formula,

$$\sum_{a\in\mathbb{Z}}f(a)=\int_{-\infty}^{\infty}dA\sum_{l\in\mathbb{Z}}f(A)\exp(2\pi iAl)\ . \tag{9}$$

Then, following the treatment of the 3D case,[12] we have

$$Z=C\int\prod_{x,i}dA_i\,\Phi(\{A\})\sum_{\{l_i\}}\prod_x\delta_{\bar\nabla_i l_i,0}\exp[-S(A,l)]\ , \tag{10}$$

$$S(A,l)=(2\beta)^{-1}\sum_x[(\nabla_2A_3-\nabla_3A_2)^2+(\nabla_3A_1-\nabla_1A_3)^2+\alpha^{-1}(\nabla_1A_2-\nabla_2A_1)^2]-2\pi i\sum_{x,i}A_il_i\ .$$

As can be seen from (8) and (9), $A_i(x)$ is a gauge field, and the functional $\Phi(\{A\})$ has been introduced to fix the gauge invariance under $A_i\to A_i+\nabla_i\lambda(x)$. The integer link variables l_i describe conserved currents ($\bar\nabla_iL_i=0$) coupled to A_i. They can be interpreted as line elements of vortex loops on the lattice. Actually one may establish the relation

$$l_i=\epsilon_{ijk}\nabla_jn_k(x+i)\ , \tag{11}$$

at the level of stationary points. In the continuum terminology, n_i of (5) measure $\int dx_i\partial_i\theta$, hence l_i counts the vorticity $\int d\theta$ around a plaquette in the (j,k) plane. By integrating over A_i, we arrive at the system of such vortex elements,

$$Z=C\sum_{\{l_i\}}\prod_x\delta_{\bar\nabla_i l_i,0}\exp[-S(l)]\ ,\qquad S(l)=4\pi^2\beta\tfrac{1}{2}\sum_{x,x'}l_i(x)V_{ij}(x,x')l_j(x')\ , \tag{12}$$

where the potential $V_{ij}(x,x')$ between two line elements is a diagonal matrix with elements given by

$$V_{ij}(x,x')=\mathrm{diag}(\alpha,\alpha,1)V(x-x') ,$$
$$V(x-x')=\int_{-\pi}^{\pi}\frac{d^3k}{(2\pi)^3}\frac{e^{ik(x-x')}}{[K_1^2+K_2^2+\alpha K_3^2]} , \quad (13)$$
$$K_i^2\equiv 2(1-\cos k_i) .$$

Z reduces to the correct expressions in the limits of $\alpha=0,1$, owing to the α dependence of $V(x)$. In particular, at $\alpha=0$ only the line elements l_3 survive and interact, within each plane, through a logarithmic potential (there is no interplane interaction). Note that similar expressions have been derived in Ref. 13 for a 2D system with continuous imaginary time, describing its quantum statistics.

For the later discussion it is useful to establish a relation with the cosine form of the XY model which is obtained by replacing S_V in (5) by

$$S_{\cos}\equiv -\beta_{\cos}\sum_x[\cos(\nabla_1\theta)+\cos(\nabla_2\theta)+\alpha_{\cos}\cos(\nabla_3\theta)] . \quad (14)$$

The b-loop representation corresponding to (7) is then obtained by replacing

$$(2\pi\beta)^{-3/2}\alpha^{-1/2}\rightarrow I_0(\beta_{\cos})^2 I_0(\alpha_{\cos}\beta_{\cos}) ,$$
$$\exp(-b^2/2\beta)\rightarrow I_b(\beta_{\cos})/I_0(\beta_{\cos}) , \quad (15)$$
$$\exp(-b^2/2\alpha\beta)\rightarrow I_b(\alpha_{\cos}\beta_{\cos})/I_0(\alpha_{\cos}\beta_{\cos}) ,$$

where $I_b(\beta_{\cos})$ are modified Bessel functions. Following an argument given in Ref. 8, we may equate the first nontrivial Fourier components ($b_l=\pm 1$) to obtain

$$\exp(-1/2\beta)=\frac{I_1(\beta_{\cos})}{I_0(\beta_{\cos})} ,$$
$$\exp(-1/2\alpha\beta)=\frac{I_1(\alpha_{\cos}\beta_{\cos})}{I_0(\alpha_{\cos}\beta_{\cos})} . \quad (16)$$

This defines a locus $\beta=\beta(\beta_{\cos}),\alpha=\alpha(\alpha_{\cos},\beta_{\cos})$ in the β-α plane, say, along which the two XY model forms become almost identical over a wide temperature range, including the critical points.

III. THEORETICAL ANALYSIS

A. Renormalization-group and scaling argument

One of the main interests in the intermediate region, $0<\alpha<1$, is to calculate the α dependence of the critical temperature $T_c(\alpha)$. The shift $T_c(\alpha)-T_{\mathrm{KT}}$ has been estimated in Ref. 14 for small α by using renormalization-group (RG) and scaling arguments. For later discussion it is useful to review it here. For small α and high temperatures, the (XY) planes are essentially decoupled, and ξ and χ behave as in a pure 2D system. As T_{KT} is approached from higher T's, larger and larger clusters of correlated spins will grow. These may be considered as block spins with an effective interaction in the z direction given by

$$J_3^{\mathrm{eff}}\simeq\alpha J\langle|C|\rangle , \quad (17)$$

where $\langle|C|\rangle$ is the average size (area) of clusters. The crossover into 3D behavior takes place around $J_3^{\mathrm{eff}}\simeq J$, i.e.,

$$\alpha\langle|C|\rangle\simeq 1 . \quad (18)$$

Hikami and Tsuneto[14] then employed the relation $\langle|C|\rangle\simeq\xi^2=\xi_0^2\exp[2b_\xi/\sqrt{T-T_{\mathrm{KT}}}]$ to derive the crossover temperature $T_\chi(\alpha)$,

$$T_\chi(\alpha)-T_{\mathrm{KT}}\simeq\frac{4b_\xi^2}{[\ln(\hat{\xi}_0^2\alpha)]^2}\propto\frac{1}{(\ln\alpha)^2} , \quad (19)$$

where we have gathered all numerical constants in $\hat{\xi}_0$. Assuming that $T_c(\alpha)\simeq T_\chi(\alpha)$, this implies the desired estimate of $T_c(\alpha)$.

Let us make a few comments on this estimate. Although we agree with the final $1/(\ln\alpha)^2$ law, one should use the relation $\langle|C|\rangle=\kappa\chi/\beta$ (κ is a constant) to estimate $\langle|C|\rangle$, which is known to be valid for the stochastically defined clusters in the Ising model [with $\kappa=1$ (Ref. 15)], and to be satisfied very well numerically for the 2D XY model [with $\kappa\simeq 0.8$ (Ref. 15)]. Since both ξ^2 and $\chi\simeq\xi^{2-\eta}$ exhibit an exponential behavior in the 2D XY model, this yields the same estimate (19), apart from the replacements $4b_\xi^2\rightarrow b_\chi^2=(2-\eta)^2 b_\chi^2$ and $\hat{\xi}_0^2\rightarrow\hat{\chi}_0^2$.

For a model with a conventional critical point governed by power-law singularities $\xi\simeq t^{-\nu},\chi\simeq t^{-\gamma}$ (e.g., the Ising model), our estimate yields the power deviation

$$T_\chi(\alpha)-T_c(0)\simeq\alpha^{1/\gamma} , \quad (20)$$

in agreement with general scaling analyses.[16] Using $\langle|C|\rangle\simeq\xi^2$ as in Ref. 14, on the other hand, would have resulted in a different power law $\simeq\alpha^{1/2\nu}=\alpha^{1/(\gamma+\eta\nu)}$. Notice that the XY-model behavior (19) can partly be recovered from (20) by taking the "infinite order" limit $\gamma\rightarrow\infty$, yielding α^0 and thus suggesting some logarithmic behavior.

Let us also give a remark for the nonlinear O(3) σ (Heisenberg) model, which is considered to describe the antiferromagnetic behaviors of high-temperature superconducting materials. It has the transition temperature $T_c(0)=0$, and $\xi\simeq\exp(b_\xi/T),\chi\simeq\exp(b_\chi/T)$.[17] Using these properties, a similar estimate gives rise to

$$T_c(\alpha)\simeq T_\chi(\alpha)\propto\frac{1}{|\ln\alpha|} . \quad (21)$$

This is in accord with one-loop RG calculations[18] (which are simpler in this case, since $T_c(0)=0$, so that a perturbative calculation becomes applicable).

Let us finally discuss the precise meaning of α in (17)–(19). Since the coupling J between spins referred to in Eq. (17) is clearly the coefficient of $\mathbf{s}_i\cdot\mathbf{s}_j$, in this subsection α should have been that in the cosine form, $\alpha_{\cos}$. For small $\alpha_{\cos}$, the mapping (16) gives the relation

$$|\ln\alpha_{\cos}|\simeq\frac{1}{\alpha} . \quad (22)$$

This logarithmic mapping generates a dramatic consequence, since upon inserting it into (19) we find for the Villain model,

$$T_X(\alpha)-T_{KT}\propto\alpha^2 \ . \tag{23}$$

In the Villain model we thus expect a smooth approach of $T_c(\alpha)$ to $T_{KT}\simeq 1/0.73$ as $\alpha\to 0$.

B. Approximate self-duality

In Ref. 19 a method has been presented for estimating the transition point β_c for $\alpha=1$. It is based on the duality between the two loop-gas representations (7) and (12) if the potential in (13) is approximated by its value at the origin. A similar approximate self-duality (ASD) argument can be applied to our case to find β_c for each α. Explicitly it leads to the following relation:

$$\frac{1}{2\beta}=2\pi^2\beta\alpha V(0) \ , \tag{24}$$

with $V(0)$ being the α dependent potential in Eq. (13). Note that the α dependences appear in such a way that the single condition (24) is sufficient to realize ASD for all three directions simultaneously. The curve of (24) is drawn in Fig. 1.

C. Migdal renormalization group

Here we shall use Migdal's recursion[20] to examine the RG trajectory of the system for general values of α to get an overview of the crossover phenomena.

Let us consider the renormalization-group equation of the model (5). We generalize the Migdal recursion equation[20] to systems having anisotropic couplings. Hence our parameter α is regarded as an effective (running) coupling constant. If we introduce the lattice spacing vector

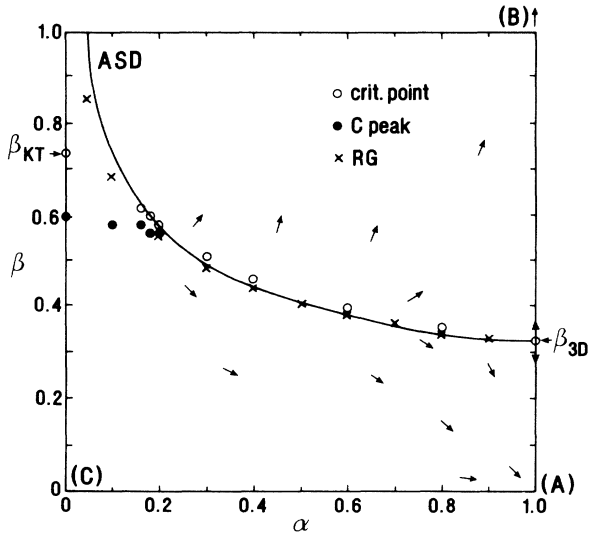

FIG. 1. Phase diagram in the α-β plane. The continuous line shows the critical points estimated by the approximate self-duality (ASD). The symbols (○) and (●) are the critical points and specific-heat maxima determined from Monte Carlo (MC) simulations with $L=16$. The symbols (×) are the critical points given by the Migdal renormalization group (RG). The arrows illustrate typical flows of RG into the infrared region.

$\mathbf{a}$, the partition function can be written in the following form:

$$Z=\int\prod_x d\theta(x)F_{\mathbf{a}}(\nabla_1\theta)F_{\mathbf{a}}(\nabla_2\theta)G_{\mathbf{a}}(\nabla_3\theta) \ . \tag{25}$$

Here we have introduced effective local Boltzmann factors F for the (1,2) direction and G for the 3 direction. Reflecting the O(2) symmetry of the system they are periodic functions and can therefore be expanded into Fourier series

$$\begin{aligned} F_{\mathbf{a}}(\varphi)&=\sum_{b\in Z} f_{\mathbf{a}}(b)\exp(ib\varphi) \ , \\ G_{\mathbf{a}}(\varphi)&=\sum_{b\in Z} g_{\mathbf{a}}(b)\exp(ib\varphi) \ . \end{aligned} \tag{26}$$

To obtain recursion equations from the spacing a to λa, we consider the Ginzburg-Landau expansion with a complex order-parameter field $\phi(x)$, corresponding to our system,

$$\begin{aligned} Z_{GL}&=\left[\prod_x\int d\phi(x)d\phi^*(x)\right]\exp(-S_{GL}) \ , \\ S_{GL}&=\int d^3x[|\partial_1\phi|^2+|\partial_2\phi|^2+\alpha|\partial_3\phi|^2+m^2|\phi|^2+g|\phi|^4] \ . \end{aligned} \tag{27}$$

Note the α in front of $|\partial_3\phi|^2$. Upon rescaling,

$$x_3'=\alpha^{-1/2}x_3 \ , \tag{28}$$

this becomes $\alpha|\partial_3\phi|^2=|\partial_3'\phi|^2$, and the action S_{GL} simplifies to a symmetric one in terms of the (x_1,x_2,x_3') coordinates. For such a symmetric system, Migdal recursions are written down with all three scaling factors $\lambda_1,\lambda_2,\lambda_3$ being set equal to λ. This means that, for the original (x_1,x_2,x_3) coordinates, we should choose λ_3 to be

$$\lambda_3=\lambda_{\text{eff}}(\alpha)\equiv 1+\sqrt{\alpha}(\lambda-1) \ , \tag{29}$$

as read from (28). Then the critical properties should be unchanged. Explicitly the recursion equations from the lattice vector $\mathbf{a}=(a,a,a_3)$ to $\mathbf{a}_{\text{new}}\equiv(\lambda a,\lambda a,\lambda_{\text{eff}}a_3)$ turn out to be

$$\begin{aligned} F_{\mathbf{a}_{\text{new}}}(\varphi)&=\left[\sum_{b\in Z}[f_{\mathbf{a}}(b)]^{\lambda}\exp(ib\varphi)\right]^{\lambda\lambda_{\text{eff}}} \ , \\ G_{\mathbf{a}_{\text{new}}}(\varphi)&=\left[\sum_{b\in Z}[g_{\mathbf{a}}(b)]^{\lambda_{\text{eff}}}\exp(ib\varphi)\right]^{\lambda^2} \ . \end{aligned} \tag{30}$$

From the original argument[20] one can easily identify the places at which λ is replaced by λ_{eff}. The extension to D-dimensional lattice with anisotropic couplings α_μ is straightforward. Now let us define a couple of relevant coupling constants. Actually we are interested in the renormalized (inverse) temperature $\beta(\mathbf{a})$ and the renormalized anisotropy parameter $\alpha(\mathbf{a})$, which are defined as

$$\begin{aligned} F_{\mathbf{a}}(\varphi)&=\exp[-\tfrac{1}{2}\beta(\mathbf{a})\varphi^2+O(\varphi^4)] \ , \\ G_{\mathbf{a}}(\varphi)&=\exp[-\tfrac{1}{2}\beta(\mathbf{a})\alpha(\mathbf{a})\varphi^2+O(\varphi^4)] \ . \end{aligned} \tag{31}$$

The results of our numerical study of (30) are given in Fig. 1. The line of critical points, (α_c,β_c), separates the low- and high-T phases. There are then the following

fixed points (see Fig. 1):

$$\text{(case } A\text{)}: \quad \alpha=1, \quad \beta=0 \text{ (3D high } T\text{)}, \tag{32a}$$

$$\text{(case } B\text{)}: \quad \alpha=1, \quad \beta=\infty \text{ (3D low } T\text{)}, \tag{32b}$$

$$\text{(case } C\text{)}: \quad \alpha=0, \quad \beta=0 \text{ (2D high } T\text{)}. \tag{32c}$$

Some typical renormalization flows are also shown. We observed that α remains zero when it was initially zero. For a nonzero starting value of α (>0), it is always driven into $\alpha=1$. The recursions have been initialized with the Villain action, and the scale parameter has been chosen to be $\lambda=1.6$ so that β_c at $\alpha=1$ agrees with the correct value ($\simeq 0.33$).

It has been shown[21] that the Migdal equation fails to reproduce the KT transition at $\alpha=0$. Instead, it predicts only the high-temperature phases; hence $\beta_c=\infty$ for $\alpha=0$.

D. Series expansions at high temperatures

The representation (7) is a convenient starting point for a systematic high-temperature (character) expansion. As $\beta\to 0$, large b loops are energetically suppressed by powers of $\exp(-1/\beta)$, so what one needs to do is to organize the sum over loop configurations according to the growing total length of loops, l, as

$$Z=\left[\frac{1}{\sqrt{2\pi\beta}}\right]^{2N}\left[\frac{1}{\sqrt{2\pi\beta\alpha}}\right]^{N}[1+Z_4+Z_6+\cdots+Z_l+\cdots]. \tag{33}$$

The leading contribution Z_4 comes from the elementary plaquettes with $b_i=\pm 1$, which appear in $2\times 3\times N$ positions: The factor of 2 accounts for the sign of b_i's (direction of flows), and the factor of 3 counts the directions of plaquettes. By taking the lattice anisotropy into account, we readily find

$$Z_4=N(2W^4+4W^2W_\alpha^2), \qquad W=\exp\left[-\frac{1}{2\beta}\right], \quad W_\alpha=\exp\left[-\frac{1}{2\beta\alpha}\right]=W^{1/\alpha}. \tag{34}$$

In the next order of $l=6$, there are three different shapes of loops: the "flat" (six links of successive directions having, say, 1,1,2,−1,−1,−2); the "bend" (say, 1,2,−1,3,−2,−3); and the "twist" (say, 1,3,2,−1,−3,−2). We find that

$$Z_6=N[4W^6+36W^4W_\alpha^2+4W^2W_\alpha^4]. \tag{35}$$

The enumeration of Z_8 is quite tedious, since there are already three two-dimensional and eight three-dimensional shapes that are geometrically distinguishable, and one disconnected graph. The result reads

$$Z_8=N[4W^8+220W^6W_\alpha^2+108W^4W_\alpha^4+4W^2W_\alpha^6+N(2W^8+8W^6W_\alpha^2+8W^4W_\alpha^4)]. \tag{36}$$

It is easy to check that all disconnected configurations cancel in the free energy, as they should because it is an extensive quantity.

The high-temperature expansion of χ proceeds in a similar manner. The main difference is that this time one must consider loops *and* chains, since χ is a lattice sum over spin-spin correlations, each having starting and ending points.

IV. MONTE CARLO STUDY

For a quantitative analysis we shall now present the results from Monte Carlo (MC) simulations. In Ref. 22 a MC analysis has been done to obtain the curve of critical temperature T_c as a function of α in the cosine form of the XY model. Here we present a set of MC results for the Villain form of the model, including the specific heat, the susceptibility, and the density of vortex loops.

A. MC simulation

Let us first describe the setup of our MC simulations. We used simple cubic lattices of sizes L^3 with L up to 24 and periodic boundary conditions. For updating the configurations, it is convenient to sum over the integer variables $n_i(x)$ in Z explicitly, and to apply the standard Metropolis algorithm only to the phase variables $\theta(x)$. We approximated them by $(2\pi/N)k, k=1,2,\ldots,N=100$. The update was organized in a checkerboard scheme to allow for efficient vectorization on a Cray X-MP supercomputer. Because of the peculiar properties of the two-dimensional XY model, a study of the crossover from the 3D behavior requires both measuring "thermal" and "magnetic" observables. For the former we have chosen the internal energy e and specific heat c (per site),

$$e=-\left[\frac{\partial}{\partial\beta}\ln Z\right]/L^3, \quad c=-\beta^2\frac{\partial}{\partial\beta}e. \tag{37}$$

The specific heat was calculated by measuring the energy fluctuations involved.[23] The "magnetic" observables are the magnetization m and the susceptibility χ (per site) defined as usual by

$$m=\langle|\vec{m}|\rangle, \quad \chi=\beta L^3[\langle\vec{m}^{\,2}\rangle-m^2], \tag{38}$$

where the angular brackets denote averages with respect to the partition function (5), and $\vec{m}\equiv\sum_x\vec{s}(x)/L^3$ is the magnetization of one configuration. To locate the transition points we found it convenient also to record the cumulant[24]

$$\kappa=1-\langle\vec{m}^{\,4}\rangle/3\langle\vec{m}^{\,2}\rangle^2, \tag{39}$$

which measures essentially the kurtosis of the spin distribution. For small β, the distribution becomes Gaussian, and κ approaches $\frac{1}{3}$, while for large β, κ tends to $\frac{2}{3}$. It is known[24] that κ exhibits a sharp crossover at the transition point β_c. This criterion for determining β_c is usually less sensitive to finite-size effects than, e.g., using the location of the susceptibility peak.

Furthermore we have measured the density and (to some extent) the distribution of the vortex lines $l_i(x)$ cal-

culated from (11) with n_i determined from minimizing $(\nabla_i\theta-2\pi n_i)^2$ at each link. (Recall that in our update procedure the n_i variables are summed over so that they are not explicitly available.) This procedure is easily seen to be equivalent to the more conventional method proposed by Tobochnik and Chester,[6] which amounts to adding up $\nabla_i\theta(\mathrm{mod}2\pi)$ around each plaquette.

Most data points are averages over 100 000 configurations, after discarding 10 000 sweeps through the lattice for thermalization. The statistical errors are estimated by dividing each run into blocks of, say, 1000, 2000, and 5000 sweeps, calculating the block averages, and taking the variance of these averages.

B. Results of MC

Let us now turn to the results of our simulations. In Fig. 1 we compare the Monte Carlo critical line in the α-β plane (denoted by circles) with those derived in the preceding sections, the continuous line determined by ASD and the crosses by Migdal recursion. In 3D($\alpha=1$) the transition point is known from previous MC calculations[7,8] to be at $\beta_c\simeq 0.33$. ASD predicts $\beta_{\mathrm{ASD}}=0.317$. In the opposite limit of 2D($\alpha=0$) the Villain model undergoes a KT transition at $\beta_{\mathrm{KT}}\simeq 0.73$.[4] It is defined as the diverging point of χ and the correlation length ξ. Recently, Chui and Giri[22] have performed MC simulations of the cosine form and determined several critical points of $\beta_{\cos}$ for values of $\alpha_{\cos}$ down to 0.01. We have checked that their values of critical points, when mapped into our α-β plane through the relation (16), are consistent with our values of critical points. However, we have proceeded far more into the 2D region because, according to (16), near the transition the smallest value of $\alpha=0.1$ in our simulation corresponds to $\alpha_{\cos}\simeq 0.0003$.

For all $\alpha\neq 0$, the critical behavior in the very vicinity of β_c is supposed to be governed by algebraic singularities, as in the 3D case. This can be seen, e.g., from the GL expansion (27). In the strict sense of universality, the point $\alpha=0$ is an isolated discontinuity. However, in the broader region of temperature away from the critical point, various observables are expected to show a continuous crossover from 3D-like to 2D-like behaviors as α decreases.

That this is really the case is demonstrated in Fig. 2, where the specific heat on a 10^3 lattice is plotted for various α's. Notice that our specific heat at $\alpha=0$ is $\frac{1}{2}$ bigger than in the pure 2D XY model due to the extra prefactor C in Eq. (7). Also note the discontinuity at $\beta=\infty$: $\lim_{\beta\to\infty} c(\alpha=0)=1$ while $\lim_{\beta\to\infty} c(\alpha>0)=\frac{1}{2}$. The shapes at $\alpha=0.1$ and 0.2 are very similar to that of 2D; they are clearly distinguishable from the 3D behavior with sharp peaks as observed for $\alpha\geq 0.4$. It is interesting to note that this crossover value of α accords nicely with the region of breakdown of ASD (see Fig. 1). Of course this MC crossover is lattice-size dependent. In order to estimate the finite-size effects, we have repeated the simulations for a couple of α's on lattices with L varying between 8 and 24. As an overall tendency, we observed that the size dependence increases quite rapidly with decreasing α.

In Fig. 3 we show the finite-size effects for $\alpha=0.2$. The

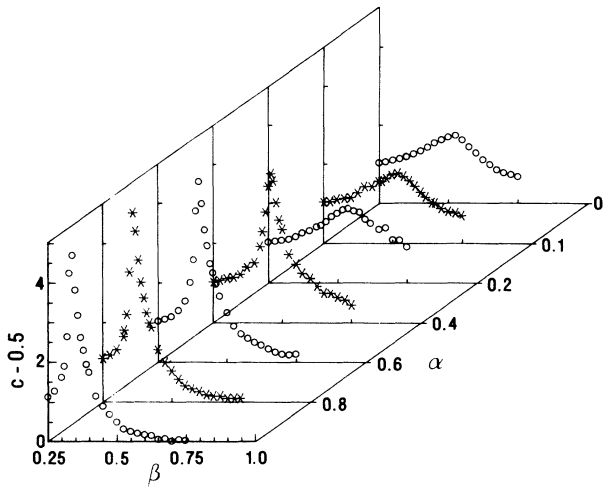

FIG. 2. Specific-heat curves on a 10^3 lattice for α varying between $\alpha=1$ (3D) and $\alpha=0$ (2D).

continuous curves in the e and c plots show the high-temperature character expansion obtained from (33)–(36) by keeping b loops of four, six, and eight links (indicated by the boxes). A similar expansion with b chains and loops with five, six, and seven links yields the susceptibility curves shown in Fig. 3(d). The MC data in Fig. 3 show quite pronounced size dependences even for the largest lattice available. From the crossing point of the cumulant curves in Fig. 3(e) we estimate $\beta_c\simeq 0.57$. For $\alpha=0.1$ the plots look similar, but the peak height of c seems to be saturated now around $c_{\max}\simeq 2.2$ for lattice sizes up to $L=24$. (Actually it is even slightly decreasing with increasing size.) The location of the peak, however, is still size dependent. It moves into lower temperatures with increasing size. This is consistent with the interpretation that, on smaller lattices, one observes apparently a KT behavior with T_{peak} displaced to higher values than T_c, while only for very large lattices can the genuine 3D-like critical behavior be seen.

The overall behavior of the crossover phenomena can be understood intuitively by referring to the vortex degree of freedom. In Fig. 3(f) the average numbers of line elements of vortex loops are shown, where M_1 (●,○) and $M_2\approx M_1$ denote the numbers of nonvanishing elements l_1,l_2 directing in the x_1 and x_2 directions, and M_3 (▲,△) denotes the number of l_3 in the x_3 direction. More and more of them are excited as the temperature increases.

In Fig. 4 snapshots of vortex configurations are displayed. For small α vortex elements along the x_3 direction appear always in pairs with small spacings and opposite directions of flow. As mentioned earlier, following Eq. (13), they can be interpreted as precursors of the 2D pointlike vortices that play the dominant role in 2D thermodynamics layer by layer. They are connected by long and complex networks of vortex lines lying within the (1,2) planes.

In Fig. 5(a) we show the variation of the ratio $R\equiv M_3/M_1$ of line-element numbers with respect to α and β. The ratio decreases, as α decreases, showing that "interplane" elements l_3 indeed become suppressed com-

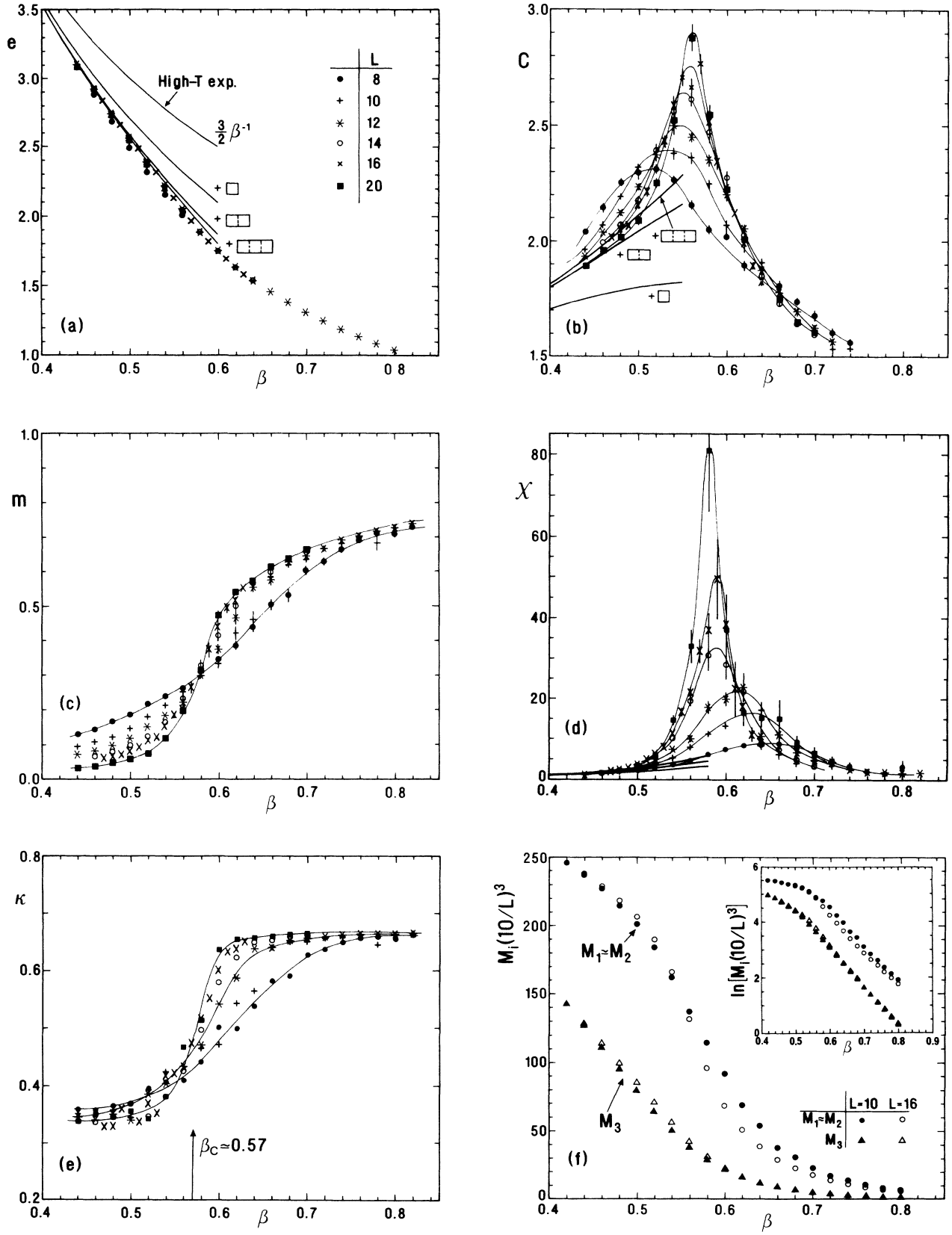

FIG. 3. Finite-size-scaling behaviors at $\alpha=0.2$ for cubic lattices with linear size L between 8 and 20. Shown are (a) internal energy e, (b) specific heat c, (c) magnetization m, (d) susceptibility χ, (e) cumulant κ [see Eq. (39)], and (f) numbers of vortex-loop line elements, $M_1 \approx M_2$ (●, ○); M_3 (▲, △). The continuous bold curves in (a), (b), and (d) show the high-temperature character expansion (33). The boxes in (a) and (b) indicate the order of this expansion. The fine curves interpolating the data are only to guide the eye.

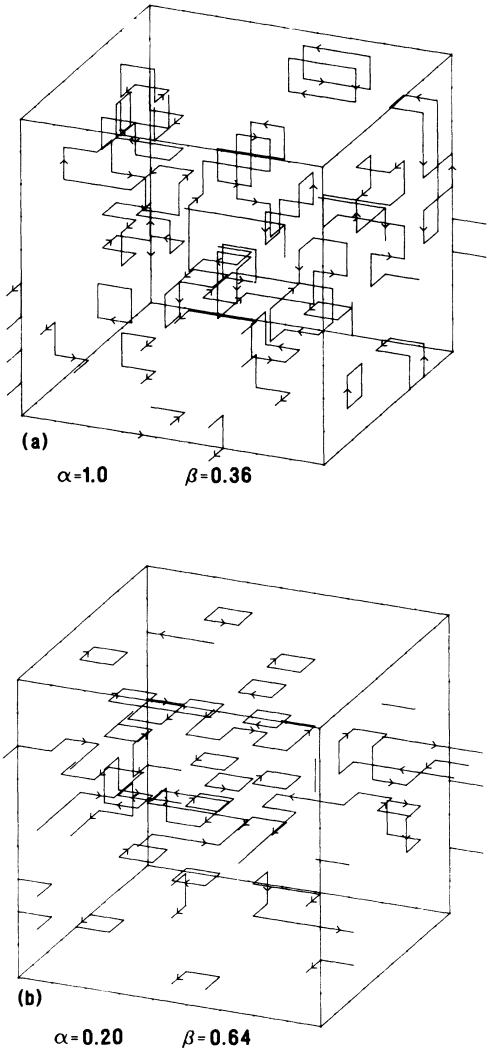

FIG. 4. Snapshots of typical vortex-loop configurations for $L=10$. (a) $\alpha=1.0, \beta=0.36$. (b) $\alpha=0.2, \beta=0.64$.

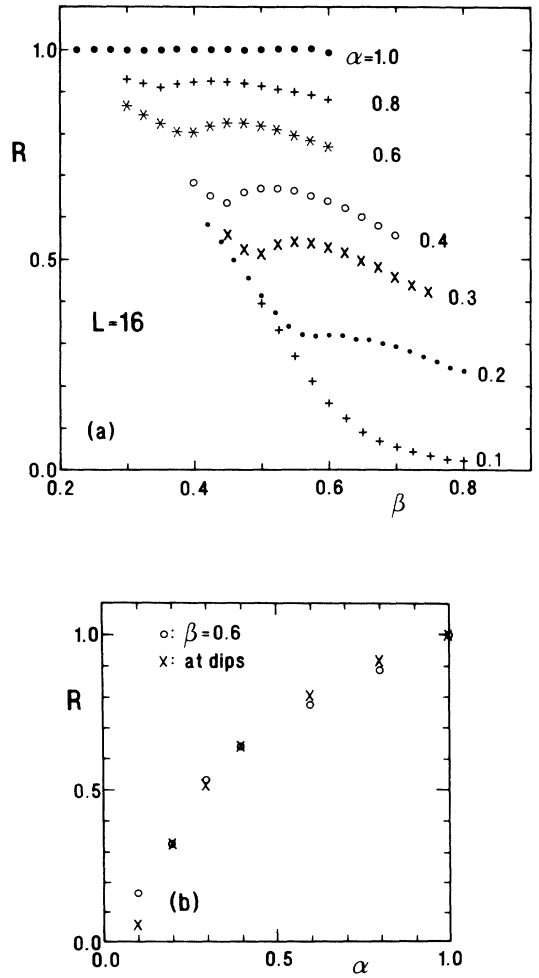

FIG. 5. (a) Ratio $R=M_3/M_1$ of vortex-loop elements. (b) The same data as in (a) replotted vs α for fixed $\beta=0.6$(○) and at the dips (×).

pared with those in the (1,2) plane. We observe that R depends on the temperature only weakly, with shallow dip near β_c. A possible explanation of these dips is as follows. For low temperatures, there are only a few closely spaced pairs of l_3 elements connected by networks of $l_{1,2}$ (see Fig. 4). As the temperature approaches the transition point, these pairs start to dissociate. While the total number M_3 is roughly fixed in this process, the total length of the connecting networks in the layers increases rapidly. As a consequence, the ratio R decreases suddenly.

In Fig. 5(b) we plot R versus α (*i*) at fixed $\beta=0.6$ and (ii) at the α-dependent transition points $\beta_c(\alpha)$ (i.e., near the dips). Again we observe a crossover behavior around $\alpha\simeq 0.1-0.2$.

V. DISCUSSION

Being motivated by recent discussions on the KT behaviors of high-T_c superconductors, we have investigated the XY model (in the Villain form) with anisotropic couplings. The overall picture that emerges from our analyses is as follows. For $\alpha>0.2$, the phase transitions are driven by a proliferation of complicated three-dimensional networks of vortex loops. With decreasing α, the line elements l_3 tends to appear in the form of pairs with opposite directions, resembling pairs of point-like vortices in two dimensions. Their interaction is governed by the potential (13), which automatically becomes logarithmic in the limit $\alpha=0$. This is in strong contrast with another mechanism, well known from magnetostatics, in which the logarithmic potential between two parallel rodlike vortex lines along the 3 direction is generated by summing over the $1/r$ potential between all line elements.

As far as the critical behaviors in the very vicinity of the transition points are concerned, the point $\alpha=0$ exhibits exponentially divergent KT behaviors and is to be distinguished from the rest ($\alpha>0$) governed by algebraic divergences. The phase transition is of second order for all $\alpha>0$. Still, the shapes of many observables show a smooth crossover into their 2D forms around $\alpha=0.1\sim 0.2$. Preliminary analyses of the finite-size effects have indicated that they become more pronounced

for smaller α.

Concerning the global structure of the α dependence of the specific heat C, we understand the following behavior to be most natural and consistent with our MC simulation. The location of the power singularity and the location of the maximum may be two independent quantities. While they seem to coincide at 3D, they follow two different lines as α decreases. The power singularity will eventually be converted into an essential singularity in the very end at 2D. The location of the maximum, on the other hand, will be smoothly connected with the KT peak in 2D. It is important to recognize that this scenario is possible due to the finiteness of C at its cusplike power singularity, which, in turn, is supported by the negative value of its 3D critical exponent α_C in (3).

Let us finally consider some implications of our study to models of high-T_c superconductivity. We would like to point out that in determining experimental values of α for high-T_c materials one should be extremely careful in using consistent assumptions: The values of α near T_{KT} in the Villain and cosine form of the XY model differ by orders of magnitude. For example, using the vortex picture, Martin *et al.*[1] have estimated $\alpha \simeq 10^{-5}$ from the observed anisotropy of the conductivities. This corresponds to $\alpha_{\cos} \simeq 10^{-30}$, or when it is the other way around, $\alpha_{\cos} = 10^{-5}$ would yield $\alpha \simeq 0.13$. Apart from other assumptions, the vortex picture itself suggests that the Villain model is more natural, since the cosine model suffers from large renormalization effects due to the spin-vortex coupling. In any case, a consistent use of one representation is crucial for a correct estimate of α.

Finally, we hope that our results will be useful for predicting the phase properties of microscopic models of high-T_c superconductivity, which can be mapped effectively onto the anisotropic XY model.

ACKNOWLEDGMENTS

We thank Professor H. Kleinert for drawing our attention to the anisotropic XY model and for interesting discussions. The Monte Carlo calculations have been performed on the Cray X-MP at Konrad-Zuse-Zentrum für Informationstechnik Berlin.

[1] P. C. E. Stamp, L. Forro, and C. Ayache, Phys. Rev. B **38**, 2847 (1988); S. Martin, A. T. Firoy, R. M. Fleming, G. P. Espinosa, and A. S. Cooper, Phys. Rev. Lett. **62**, 677 (1989); **63**, 583 (1989); N.-C. Yeh and C. C. Tsuei, Phys. Rev. B **39**, 9708 (1989); S. N. Artemenko, I. G. Gorlova, and Yu. I. Latyshev, Phys. Lett. A **138**, 428 (1989).

[2] J. M. Kosterlitz and D. J. Thouless, J. Phys. C **6**, 1181 (1973); J. M. Kosterlitz, J. Phys. C **7**, 1046 (1974); V. L. Berezinskii, Zh. Eksp. Teor. Fiz. **61**, 1144 (1971) [Sov. Phys. JETP **34**, 610 (1972)]; P. Minnhagen, Rev. Mod. Phys. **59**, 1001 (1987).

[3] J. Villain, J. Phys. (Paris) **36**, 581 (1975).

[4] W. J. Shugard, J. D. Weeks, and G. H. Gilmer, Phys. Rev. Lett. **41**, 1399 (1978); **41**, 1577(E) (1978); see also W. Janke and H. Kleinert, Phys. Rev. B **41**, 6848 (1990).

[5] R. Gupta, J. DeLapp, G. G. Batrouni, G. C. Fox, C. F. Baillie, and J. Apostolakis, Phys. Rev. Lett. **61**, 1996 (1988).

[6] J. Tobochnik and G. V. Chester, Phys. Rev. B **20**, 3761 (1979).

[7] C. Dasgupta and B. I. Halperin, Phys. Rev. Lett. **47**, 1556 (1981).

[8] W. Janke and H. Kleinert, Nucl. Phys. **B270**, [FS10] 135 (1986).

[9] M. Ferer, M. A. Moore, and M. Wortis, Phys. Rev. B **8**, 5205 (1973).

[10] J. A. Lipa and T. C. P. Chui, Phys. Rev. Lett. **51**, 2291 (1983); K. H. Mueller, G. Ahlers, and F. Pobell, Phys. Rev. B **14**, 2096 (1976).

[11] J. C. Le Guillou and J. Zinn-Justin, Phys. Rev. Lett. **39**, 95 (1977); Phys. Rev. B **21**, 3976 (1980).

[12] R. Savit, Rev. Mod. Phys. **52**, 453 (1980).

[13] H. Kleinert, Int. J. Eng. Sci. **23**, 927 (1985).

[14] S. Hikami and T. Tsuneto, Prog. Theor. Phys. **63**, 387 (1980).

[15] U. Wolff, Phys. Rev. Lett. **62**, 361 (1989); Nucl. Phys. **B322**, 759 (1989).

[16] R. Abe, Prog. Theor. Phys. **44**, 339 (1970); A. Hankey and H. E. Stanley, Phys. Rev. B **6**, 3515 (1972); L. L. Liu and H. E. Stanley, *ibid.* **8**, 2279 (1973).

[17] A. M. Polyakov, Phys. Lett. **59B**, 79 (1975); E. Brézin and J. Zinn-Justin, Phys. Rev. B **14**, 3110 (1976).

[18] H. Yamamoto, G. Tatara, I. Ichinose, and T. Matsui (unpublished).

[19] T. Banks, R. Myerson, and J. Kogut, Nucl. Phys. **B129**, 493 (1978).

[20] A. A. Migdal, Zh. Eksp. Teor. Fiz. **69**, 810 (1975) [Sov. Phys. JETP **42**, 413 (1976)]; L. P. Kadanoff, Rev. Mod. Phys. **49**, 267 (1977).

[21] K. R. Ito, Phys. Rev. Lett. **54**, 2383 (1985).

[22] S. T. Chui and M. R. Giri, Phys. Lett. A **128**, 49 (1988).

[23] There is an unusual extra term in c since, after summing over n_l, the effective energy in (5) is β dependent.

[24] K. Binder, Z. Phys. B **43**, 119 (1981).